Challenges in fuel cell power plant control: The role of system level dynamic models

Subbarao Varigonda Jay T. Pukrushpan Anna G. Stefanopoulou

January 10, 2003

Abstract

Fuel cells permit clean and efficient energy production for stationary and transportation applications. One of the most promising fuel cell power plant technologies is the Polymer Electrolyte (or Proton Exchange) Membrane Fuel Cell (PEM-FC) coupled to a fuel processor. The Fuel Processing System (FPS) reforms a hydrocarbon fuel like natural gas into a hydrogen rich feed for the fuel cell. Cost and performance requirements of the power plant typically lead to highly integrated designs and stringent control objectives.

System level dynamic models of fuel cell power plants built from physics based component models are extremely useful in understanding the system level interactions, implications on system performance and in model-aided controller design. System level dynamic models also help in evaluating alternative system architectures in an integrated design & control paradigm. We illustrate the ideas using two control problems: 1) the coordination of fuel and air flows into the FPS for load tracking and reformer temperature control and 2) implications of sensor selection in estimating critical FPS performance variables.

1 Introduction

A PEM fuel cell connected with a natural gas fuel processor is considered in this paper. The fuel processor converts the natural gas to a hydrogen (H_2) rich mixture that is directly feed to the PEM-FC. The natural gas fuel processing system (FPS) is composed of four main reactors, namely, hydro-desulfurizer (HDS), catalytic partial oxidation (CPOX), water gas shift (WGS) and preferential oxidation (PROX) as shown in Fig. 1.

Sulfur is first removed from the natural gas (mostly methane CH_4) stream in the HDS. Then the gas steam is mixed with atmospheric air and then reacts in the CPOX to produce hydrogen-rich gas. The WGS and the PROX reactors are then used to clean up carbon monoxide (CO) that is created in the CPOX. We assume here

*This work is supported by the National Science Foundation under contracts CMS-0201332 and CMS-0219623 and a fellowship from the Royal Thai Government. Varigonda is with United Technologies Research Center. J. T. Pukrushpan and A. G. Stefanopoulou are with the Department of Mechanical Engineering, University of Michigan, Ann Arbor, MI 48109 USA.

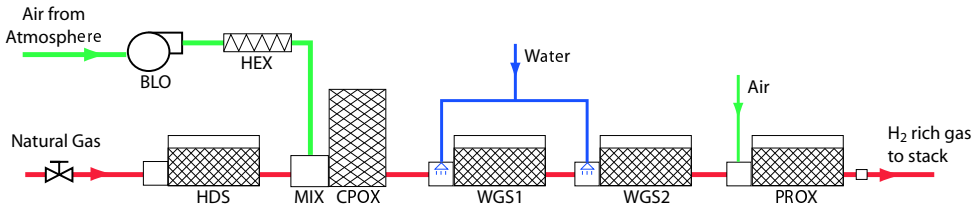

Figure 1: FPS Components

perfect CO conversion at the WGS and the PROX which we call from now on as WROX (=W[$GS + P$]ROX). The control-oriented dynamic model, however, accounts for the effects of the added partial pressure from the vapor and air flow introduced within the WROX stages of the FPS. Consequently, the amount of hydrogen created in the FPS depends solely on the supply rate of CH_4 and the CPOX air to fuel ratio, more specifically, oxygen to carbon ratio ($, _{O2C}$). This oxygen to carbon ratio also influences the amount of heat generated in the CPOX, which then affects the CPOX catalyst bed temperature. During changes in the stack current, the fuel processor needs to quickly replenish the amount of hydrogen in the fuel cell stack (anode) while maintaining the desired temperature of the CPOX catalyst bed.

There are, thus, two control objectives. First, to prevent stack H_2 starvation, or fuel starvation [1, 2], which can permanently damage the stack. To this end, the hydrogen flow exiting the FPS must respond fast and be robust to changes in stack power level, i.e. changes in stack current. Unfortunately, oversupply of H_2 by adjusting the FPS flow at a higher steady-state level is not an option because this will cause a lot of wasted hydrogen from the anode exit [2], and consequently, low utilization (U_{H_2}). Based on the Department of Energy (DOE) report [3] both utilization and starvation depend on the hydrogen mole fraction (y_{H_2}) exiting from the stack. Thus, the hydrogen generation needs to be following the current load in a precise and fast manner to maintain a reasonably low level of y_{H_2}.

Second, the temperature of the CPOX, T_{cpox}, must be maintained at certain level. Exposed to high temperature will permanently damage the CPOX catalyst bed while low CPOX temperature slows down the CH_4 reaction rate [4]. This is achieved indirectly by accurate control of the $, _{O2C}$ in the CPOX, and thus, it requires coordination of the fuel value (natural gas valve, u_{valve}) and the blower command (u_{blo}) for the correct mixture at the catalyst bed.

In the following sections, we demonstrate how control theoretic tools can be used to analyze necessary tradeoffs between the two control objectives, and thus, guide the controller and system design. Moreover, we demonstrate how simple linear observability analysis can facilitate decisions on sensor selection.

2 Control Model Assumptions and Range of Validity

The model of the FPS is developed with a focus on the dynamic behaviors associated with the flows and pressures in the FPS and also the temperature of the CPOX. We assume that the distributed nature of the stack starvation and the catalyst temperature can be lumped in spatially averaged variables and described using ordinary differential equations. Figure 2 illustrates the simplified system and state variables used in the model.

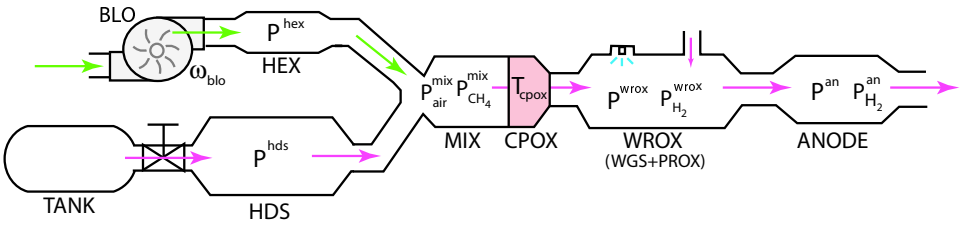

Figure 2: FPS Dynamic Model

The de-sulfurization process in the HDS is not modeled and thus the HDS is viewed as a storage volume. It is also assumed that both the WGS and PROX (here called for simplicity the WROX) are perfectly controlled such that the desired values of the reactants are supplied to the reactors. It is assumed that the composition of the air entering the FPS is constant. Additionally, any temperature other than CPOX temperature is assumed constant and the effect of temperature changes to pressure dynamics is assumed negligible. All gases, obey the ideal gas law and all gas mixtures are prefect mixtures.

The volume of CPOX is relatively small and is thus ignored. It is assumed that all CH_4 reacts if sufficient oxygen is supplied to the CPOX. The rate of CPOX reactions does not depend on CPOX temperature or reactant concentration. It depends only on the oxygen to carbon ratio in the CPOX.

The low-order (11 states) model described in the previous section is parameterized and validated with the results of a high-order (> 300 states) detailed fuel cell system model [5] which was developed in Modelica language using Dymola software [6]. The focus is on representing dynamic behaviors, and, thus, reasonable agreement of transient responses is the main concern. Several parameters such as orifice constants and component volumes are adjusted appropriately in order to obtain comparable transient responses. Note that the model is expected to provide close prediction of transient response for variables located upstream from the WGS inlet (WROX inlet). The responses of the performance variables are shown in Figure 3. The right column are the zoom-in of the response at 1600 second which represents simultaneous input step increase. It can be seen that, despite the offset, there is a good agreement in most transient responses between the two model.

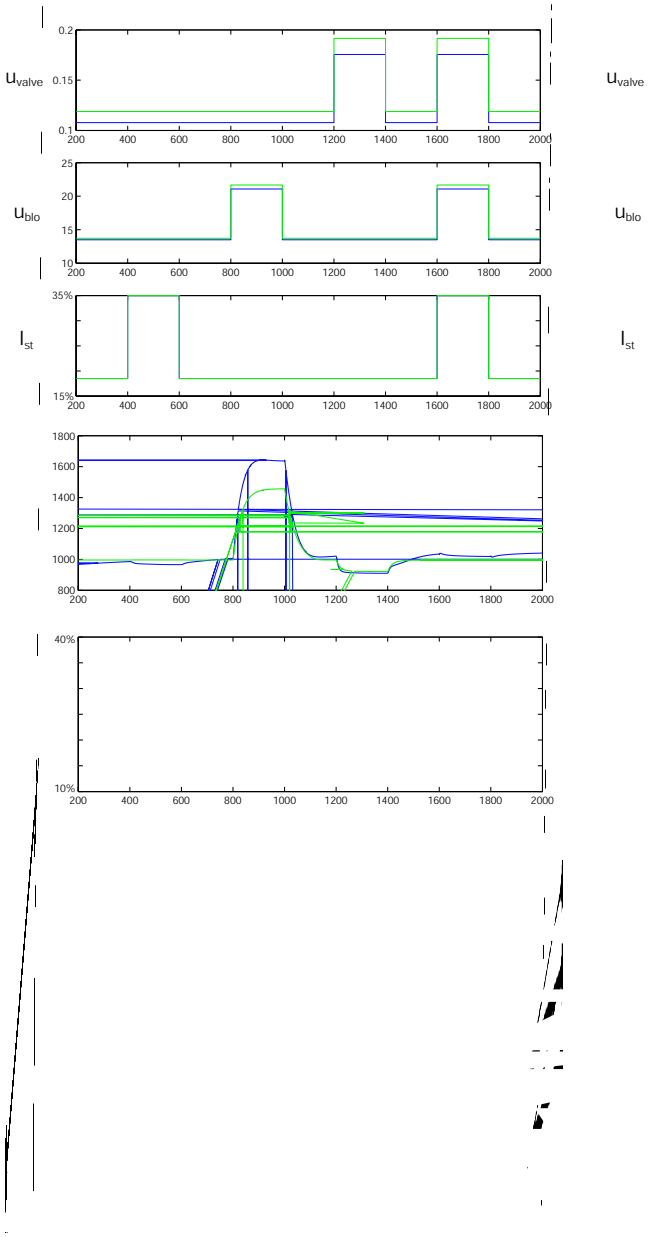

Figure 3: Model Validation Results: Inputs and Performance Variables. Blue (or dark)= High-order model. Green (or light)= Low-order model

3 Input-Output Model

Stack current, I_{st}, is considered as an exogenous input that is measured. Since the exogenous input is measured, we consider a two degree of freedom (2DOF) controller based on feedforward and feedback as shown in Figure 4. The control objective is to reject or attenuate the response of the disturbance w to the performance z by controlling the input, u, based on the measurement, y.

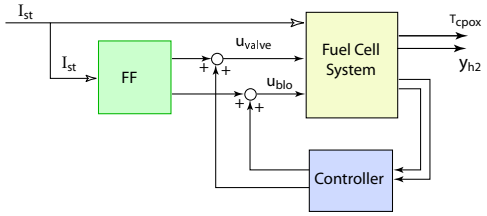

Figure 4: Feedback and Feedforward Control Architecture

The two control inputs, u, are air blower signal, u_{blo}, and fuel valve signal, u_{valve}. The performance variable, z, includes CPOX temperature, T_{cpox}, and anode exit hydrogen mole fraction, $y^{an}_{H_2}$. Several set of measured variables are considered. In order to determine the fundamental limitations or issues that are related to the plant based on the actuator topology and not the sensors, we first study the control design based on perfect measurements of the performance variables, i.e. perfect measurement of T_{cpox} and $y^{an}_{H_2}$. Then, later in this chapter, we study the effect of using realistic measurement on the control architecture and the controller performance. The actuator dynamics are neglected. The sensor dynamics are included when realistic (delayed and noisy) sensor measurements are considered.

The desired steady-state efficiency is obtained by operating the system at stack H_2 utilization, U_{H_2}=80% [7] and CPOX oxygen-to-carbon ratio, $¸_{O2C} = 0{:}6$. This condition results in the value of CPOX temperature, $T_{cpox} = 972$K as in [8] (corresponds to $¸_{O2C} = 0{:}6$) and the value of anode hydrogen mole fraction, $y^{an}_{H_2} \approx 8\%$ (corresponds to $U_{H_2} = 80\%$). The nonlinear plant model is linearized at three different current (load) levels, 30%, 50% and 80%, which will be referred to as 30%, 50% and 80% system (or model), respectively. The linearization of the plant is denoted by

$$\begin{aligned} \dot{x} &= Ax + B_u u + B_w w \\ z &= C_z x + D_{zu} u + D_{zw} w \end{aligned}$$

where x, u, w, and z are

$$\begin{aligned} x &= \begin{bmatrix} p^{wrox}_{H_2} & p^{wrox} & p^{an} & T_{cpox} & p^{an}_{H_2} & p^{mix}_{air} & p^{mix}_{CH_4} & p^{hex} & !_{blo} & p^{hds} & p^{hds}_{CH_4} \end{bmatrix}^T \\ w &= I_{st} \qquad u = \begin{bmatrix} u_{blo} & u_{valve} \end{bmatrix}^T \qquad z = \begin{bmatrix} T_{cpox} & y^{an}_{H_2} \end{bmatrix}^T \end{aligned} \tag{1}$$

In transfer function form, we can represent the plant as

$$\begin{bmatrix} z \\ y \end{bmatrix} = G \begin{bmatrix} w \\ u \end{bmatrix} = \begin{bmatrix} G_{zw} & G_{zu} \\ G_{yw} & G_{yu} \end{bmatrix} \begin{bmatrix} w \\ u \end{bmatrix} \tag{2}$$

and apply theoretical tools to determine the appropriate feedback control architecture.

4 Input-Output Pairing

The open loop response of the linear system is shown in Fig. 5. The output are in the units as follows:$y_{H_2}^{an}$ (%) and T_{cpox} (K). For clarity, in these two figures, the units of current is (decaAmp $=\times 10$ Amp).

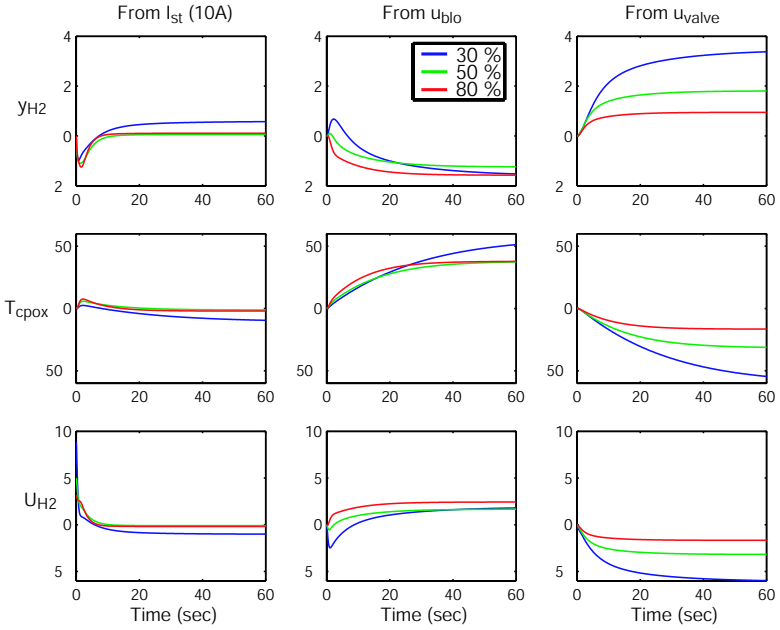

Figure 5: Step responses of linearized models at 30%, 50% and 80% power

Note first that the feedforward controller does well in rejecting the effect from I_{st} to y_{H_2} and U_{H_2} in steady state. The steady-state cancellation is perfect at the 50% load because the feedforward terms have been designed for the 50% load. The feedforward H_2 starvation recovers, however, relatively slow. A feedback controller is, thus, needed to speed up the system behavior and reduce the sensitivity introduced by modelling uncertainty.

The responses of the output due to step changes in the actuator signals show a strongly coupled system. The fuel dynamics are slower than the air dynamics, primarily due to the large HDS volume. Unfortunately, the fast air dynamics cannot be used effectively to improve starvation because of the non-minimum phase behavior observed between the blower input u_{blo} to anode H_2 mole fraction.

A method used to measure the interaction and assess appropriate pairing is called Relative Gain Array (RGA)

[9]. The RGA is a complex non-singular square matrix defined as

$$RGA(G) = G \times (G^{-1})^T \tag{3}$$

where $\times$ denotes element by element multiplication. Each element of RGA matrix indicates the interaction between the corresponding input-output pair. It is preferred to have a pairing that give RGA matrix close to identity matrix. The useful rules for pairing are [10]

1. To avoid instability caused by interactions at low frequencies one should *avoid* pairings with negative steady-state RGA elements.
2. To avoid instability caused by interactions in the crossover region one should *prefer* pairings for which the RGA matrix in this frequency range is close to identity.

The RGA matrices of G_{zu} of 50% system at steady-state is given in (4). According to the first rule, it is clear that the preferred pairing choice is $u_{blo} \rightarrow T_{cpox}$ pair and $u_{valve} \rightarrow y_{H_2}$ pair to avoid instability at low frequencies.

$$RGA(0 \text{ rad/s}) = \begin{bmatrix} 2.346 & -1.346 \\ -1.346 & 2.346 \end{bmatrix} \tag{4}$$

However, it can be seen that at high frequencies, the diagonal and off-diagonal elements are closer which indicates more interactions. In fact, the plot of the difference between the diagonal and off-diagonal elements of RGA matrices of the linearized systems at 30%, 50% and 80% power in Figure 6 shows that the interactions increase at high frequency. At low power level, the value of the off-diagonal element of RGA matrix is even higher than the diagonal element ($RGA_{11} - RGA_{12} < 0$) indicates large coupling in the system. At these frequencies, we can expect poor performance from a decentralized controller.

Consequently, one should expect that fast controllers cannot be used for both loops because the control performance starts deteriorating due to system interactions. Moreover, since the interaction is larger for the low power (30%) system, the performance of fast decentralized control deteriorates significantly and can even destabilize the system. To prevent the deteriorating effect of the interactions, it is possible to design the two controllers to have different bandwidth. Therefore, to get fast y_{H_2} response while avoiding the effect of the interactions, the T_{cpox}-air loop needs to be slow. This compromise is not necessary for a multivarible controller that coordinates both actuators based on the errors in both performance variables.

5 Sensors and Observability Analysis

We first assume perfect measurements of T_{cpox} and y_{H_2} [11]. The linearized open loop system becomes

$$\begin{aligned} \dot{x} &= Ax + B_u u + B_w w \\ y = z &= C_z x + D_{zu} u + D_{zw} w: \end{aligned} \tag{5}$$

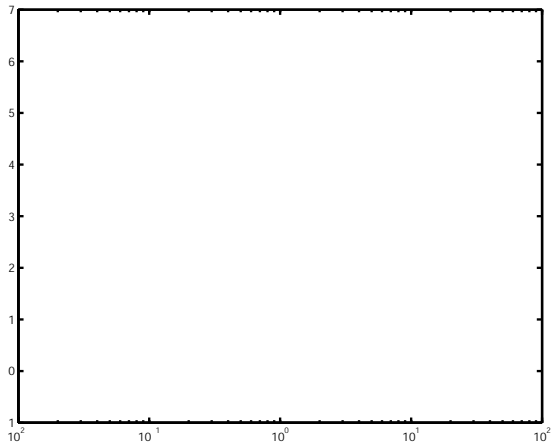

Figure 6: Difference between diagonal and off-diagonal elements of the RGA matrix at different frequencies for three linearized model

The observability matrix $O(A; C_z)$ has full rank and thus it is possible to build the estimator using only these two measurements. However, the condition number of the observability gramian,Q_{obs}, i.e. solution of

$$A^T Q_{obs} + Q_{obs} A = -C_z^T C_z; \tag{6}$$

is high. To better evaluate the system observability we normalize the observability gramian (NQ_{obs})

$$NQ_{obs} = \frac{\text{cond } (Q_{obs}; _{\{C=C_z\}})}{\text{cond } (Q_{obs}; _{\{C=I\}})} = 1{:}81 \times 10^6{:} \tag{7}$$

Large normalized observability gramian indicates that $(A;\ C_z)$ pair is weakly observable.

In practice, the CPOX temperature measurement and anode hydrogen mole fraction can not be instantaneously measured. The temperature and hydrogen sensors are normally slow, with time constants of approximately 60 seconds and 20 seconds, respectively. The lag in the measurements degrades further the estimator performance and thus the feedback bandwidth is detuned in favor of robustness. For fast response, the system has to rely more on feedforward control of the fuel valve and the blower command based on the measured exogenous input, I_{st}. The feedforward controller, in turn, depends on the actuator response and reliability. A common method to speed up and robustify the actuators performance is a cascade configuration of a 2DOF controller for each actuator based on measurement of the air flow rate, W_{air} and the fuel flow rate, W_{fuel} (both in g/sec).

Each set of measurements provides different degree of observability as can be seen by comparing the normalized condition number of the observability gramian in Table 1. The lag contributed by the sensors significantly degrades the system observability. However, adding the fuel and air flow measurements lowers the observability condition number to a value lower than the one obtained with perfect measurement of T_{cpox} and y_{H_2}. We can, thus, expect a better estimation performance. Even better estimation can be expected if additional measurements

such as anode pressure are available as shown in the table below. More work is needed to define the critical measurements that will be beneficial for the combined observer-based controller.

Table 1: Normalized Condition number of observability gramian

Measurements	NQ_{obs}
T_{cpox}, y_{H_2}	$1{:}81 \times 10^{6}$
T^m_{cpox}, $y^m_{H_2}$	$3{:}037 \times 10^{12}$
T^m_{cpox}, $y^m_{H_2}$, W_{air}, W_{fuel}	$7{:}657 \times 10^{4}$
T^m_{cpox}, $y^m_{H_2}$, W_{air}, W_{fuel}, p^{an}	$5{:}982 \times 10^{3}$

6 Concluding Remarks

Control theoretic tools such as the relative gain array (RGA) and the observability gramian are employed to guide the control design for a FPS combined with a PEM-FC.

These tools provide insight about the subsystem interactions and can point to system redesign. For example this simple MIMO analysis suggests that a decrease in HDS volume is more critical than a faster blower for the starvation control. The observability analysis can help in assessing the relative cost-benefit ratio in adding extra sensors in the system.

References

[1] W-C Yang, B. Bates, N. Fletcher, and R. Pow, "Control challenges and methodologies in fuel cell vehicle development," *SAE Paper 98C054*.

[2] R-H Song, C-S Kim, and D.R. Shin, "Effects of flow rate and starvation of reactant gases on the performance of phosphoric acid fuel cells," *Journal of Power Sources*, vol. 86, pp. 289–293, 2000.

[3] R.S. Glass, "Sensor needs and requirements for fuel cells and CIDI/SIDI engines," Tech. Rep., Department of Energy, April 2000, Published by Lawrence Livermore National Laboratory.

[4] J. Zhu, D. Zhang, and K.D. King, "Reforming of CH_4 by partial oxidation: thermodynamic and kinetic analyses," *Fuel*, vol. 80, pp. 899–905, 2001.

[5] J. Eborn, L.M. Pedersen, C. Haugstetter, and S. Ghosh, "System level dynamic modeling of fuel cell power plants," *to be presented in 2003 American Control Conference*, 2003.

[6] Michael Tiller, *Introduction to Physical Modeling with Modelica*, Kluwer Academic Publishers, Boston, 2001.

[7] E.D. Doss, R. Kumar, R.K. Ahluwalia, and M. Krumpelt, "Fuel processors for automotive fuel cell systems: a parametric analysis," *Journal of Power Sources*, vol. 102, pp. 1–15, 2001.

[8] C.R.H. de Smet, M.H.J.M. de Croon, R.J. Berger, G.B. Marin, and J.C. Schouten, "Design of adiabatic fixed-bed reactors for the partial oxidation of methane to synthesis gas. application to production of methanol and hydrogen-for-fuel-cells," *Chemical Engineering Science*, vol. 56, pp. 4849–4861, 2001.

[9] E.H. Bristol, "On a new measure of interactions for multivariable process control," *IEEE Transactions on Automatic Control*, vol. AC-11, pp. 133–134, 1966.

[10] Sigurd Skogestad and Ian Postlethwaite, *Multivariable Feedback Control: Analysis and Design*, Wiley, 1996.

[11] The Argus Group, "Hydrogen sensor for automotive fuel cells from the argus group," *http://www.fuelcellsensor.com/*, 2001.